ACS Macro Letters

Letter

pubs.acs.org/macroletters

Nanoconfinement and Chemical Structure Effects on Permeation Selectivity of Self-Assembling Graft Copolymers

Chiara Vannucci,[†] Ikuo Taniguchi,[‡] and Ayse Asatekin*[,†]

[†]Chemical and Biological Engineering Department, Tufts University, 4 Colby Street, 02155 Medford, Massachusetts, United States

[‡]International Institute for Carbon-Neutral Energy Research (WPI-I^{2}CNER), Kyushu University 744 Motooka, Nishi-ku, Fukuoka 819-0395, Japan

Supporting Information

ABSTRACT: Permeation of small molecule solutes through thin films is typically described by the solution-diffusion model, but this model cannot predict the effects of nanostructure due to self-assembly or additives. Other models focusing on diffusion through isolated nanopores indicate that confining permeation to channels slightly larger than the size of the solute can lead to an increased influence of solute−pore wall interactions on permeation rate. In this study, we analyze how differences in polymer nanostructure affect the relative contributions of solute size and polymer−solute interactions on transport rate. We compared the diffusion rates of several small molecules through two polymer thin films: A cross-linked, homogeneous film of poly(ethylene glycol phenyl ether acrylate) (PEGPEA) and a graft copolymer with a poly(vinylidene fluoride-*co*-chlorotrifluoroethylene) (P(VDF-*co*-CTFE)) backbone and PEGPEA side chains that self-assemble into continuous ∼1−3 nm PEGPEA domains through which transport occurs. We correlated these rates with the size of each solute and its chemical affinity to PEGPEA, as measured by the difference between their solubility parameters. Diffusion rate through the homogeneous polymer film was controlled by solute size, whereas diffusion rate through the copolymer was strongly controlled by the difference between the solubility parameters. Furthermore, permeation selectivity between two selected molecules was 2.5× higher for the nanostructured copolymer, likely enhanced by the nanoconfinement effects. These initial results indicate that polymer self-assembly is a promising tool for designing polymeric membranes that can differentiate between solutes of similar size but differing chemical structures.

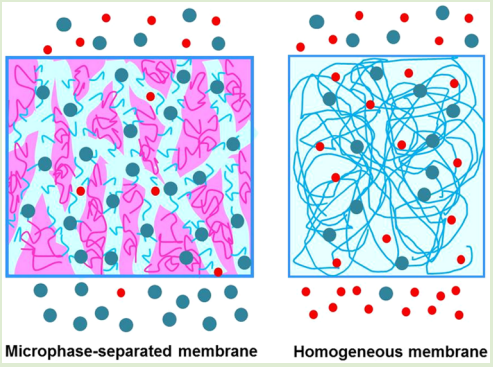

Regulating permeation through materials is crucial for many applications, including selective membranes, controlled drug delivery, and packaging.[1−7] Permeation selectivity is especially critical in membrane separations. Membranes that are capable of separating small molecules of similar size by their chemical structure can potentially have great impact in drug manufacture[8−10] and the petrochemical industry. A better understanding of how to modulate the permeation of small molecules through polymers by manipulating chemical interactions and nanostructure can open up new avenues to such membranes.

Most current membrane selective layers are homogeneous polymers[11−13] where permeation is described by the solution-diffusion model. The solute dissolves in the polymer on the feed side, diffuses, and desorbs into the permeate. The molar flux J_A of solute A through the polymer film is given by

$$J_A = S_A D_A \frac{\Delta C_A}{z} = P_A \frac{\Delta C_A}{z} \quad (1)$$

where S_A, D_A, and P_A are the solubility, diffusivity, and permeability of A in the polymer, respectively, z is the polymer film thickness, and ΔC_A is the concentration difference between the feed and permeate. The permeability of a solute increases with increasing solubility in the polymer and decreasing solute size.

This model works well for most gas separation membranes[11−14] and has been adapted for desalination.[11,13−15] However, it does not account for the effect of nanostructure observed in copolymers that microphase separate.[16,17] The importance of nanoscale structure is best observed in biological transport systems like porins,[18] nuclear pore complex,[19] and ion channels,[20] which achieve very sharp permeation selectivity through synergistic effects of pore size and molecular recognition. These pores are only slightly larger than their target molecule, lined with functional groups that selectively interact with their target. This emphasizes the effect of interactions between the solute and the functional groups within pores,[21,22] leading to the selective transport of the target molecule. Therefore, combining nanoscale confinement with specific membrane−solute interactions is the biomimetic key to developing systems that feature chemical structure based selectivity.

Received: June 15, 2015
Accepted: August 5, 2015
Published: August 6, 2015

DOI: 10.1021/acsmacrolett.5b00401
ACS Macro Lett. 2015, 4, 872−878

Most approaches to prepare nanopores lined with functional groups use top-down modification of membranes with cylindrical through-pores, for example, thiol chemisorption into gold nanotube membranes,[23,24] silane deposition, and surface-initiated polymerization on anodized aluminum oxide membranes,[25,26] polyelectrolyte deposition inside nanotubules,[27] and initiated chemical vapor deposition onto track-etched membranes.[28] However, these manufacturing methods show poor scalability and yield very low pore densities. This would lead to low productivity when used as a separation membrane.

Creating the desired functional nanostructures in a single step through polymer self-assembly circumvents these limitations.[29] Most membrane applications focus on block copolymers, which create ordered cylindrical structures that can be aligned perpendicular to the membrane surface. However, the smallest scale that can be achieved with block copolymers is around 3 nm,[30−34] much larger than small molecules. In comparison, graft copolymers can form network structures that are disordered but continuous. These do not require further alignment. The domain size is comparable with the radius of gyration of side chains,[35] down to 1 nm,[36−38] comparable with the size of small molecule solutes. The nanostructure can be controlled by modulating the copolymer architecture, composition, and molecular weight. The copolymers can be functionalized,[39−41] making it possible to create specific interactions between these chemical groups and the solutes permeating through the membrane.

Here, we aim to gain mechanistic insight into permeation through nanostructured polymers. We study how differences in polymer nanostructure affect the relative contributions of solute size and polymer-solute interactions on transport rate. For this purpose, we selected an aromatic polymer, poly(ethylene glycol phenyl ether acrylate) (PEGPEA). We compared the permeation rates of solutes through two polymer films that incorporate PEGPEA: a graft copolymer with PEGPEA side chains that self-assembles into continuous nanodomains ∼1−3 nm in diameter and cross-linked PEGPEA. We correlated the permeabilities of several solutes through these films with their chemistry and size. We have shown that the chemical structure differences have a stronger influence on selectivity in the graft copolymer due to nanoconfinement and increased solute-PEGPEA contacts, similar to that observed in nanochannels described above,[42] whereas permeability through the homogeneous cross-linked polymer is dominated by size effects. We also demonstrated that the microphase separated copolymer provides more effective separation of molecules of similar size but different chemical structure. This is, to our knowledge, the first documentation of increased permeation selectivity due to nanostructure in a self-assembled system.

The graft copolymer we studied has a polyvinylidene fluoride (PVDF) backbone that microphase separates from PEGPEA. We synthesized this copolymer by a "grafting from" approach,[43] using poly(vinylidenefluoride-*co*-chlorotrifluoroethylene), P(VDF-*co*-CTFE) (Solvay Specialty Polymers, M_n 149 kDa), as a macroinitiator for atom transfer radical polymerization (ATRP).[39,44] A Cu(I)−ligand complex abstracts chlorine atoms from CTFE units[45] that initiate the polymerization of ethylene glycol phenyl ether acrylate (EGPEA) to form the side chains. The molar ratio between VDF and CTFE in P(VDF-*co*-CTFE) was measured to be ∼11:1 by ^{19}F NMR (Figure 1a), corresponding to 14 wt % CTFE.

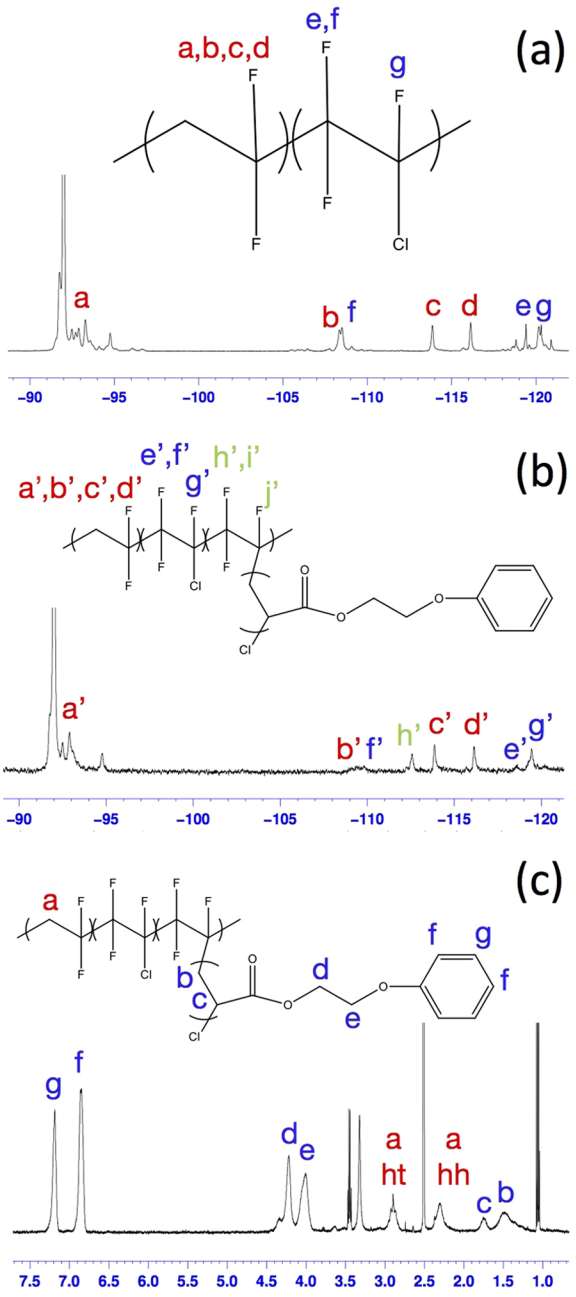

Figure 1. ^{19}F NMR of PVDF (a) and PVDF-*g*-PEGPEA (b) and ^{1}H NMR of PVDF-*g*-PEGPEA (c).

P(VDF-*co*-CTFE) was previously used as an ATRP macroinitiator,[46] but the initiation efficiency of the chlorine atoms in CTFE was not determined before. These atoms are bound relatively strongly in comparison with preferred ATRP initiators, so the initiation may not be as fast or efficient as in systems with better control. We determined the initiation efficiency from the ^{19}F NMR spectrum of P(VDF-*co*-CTFE)-*g*-PEGPEA, termed PVDF-*g*-PEGPEA for the sake of brevity (Figure 1b). The peak at −112.5 ppm, attributed to -CF_2CF(PEGPEA)$CF_2CF_2CH_2$- (h′),[47] is absent in the backbone spectrum. Using this peak and the peak at −109.5 ppm, attributed to the convolution of -$CF_2CH_2CF_2CF_2CFCl$- (b, b′) and -$CF_2CFClCF_2CFClCH_2$- (f, f′), the percentage of initiated chlorine was calculated to be 74%. Using ^{1}H NMR (Figure 1c), PVDF-*g*-PEGPEA copolymer was found to contain 70 wt %

DOI: 10.1021/acsmacrolett.5b00401
ACS Macro Lett. 2015, 4, 872−878

PEGPEA and a molecular weight of 500 kDa. Each side chain consists of, on average, 10 EGPEA units.

The PVDF-*g*-PEGPEA copolymer was designed to form a continuous network of PEGPEA nanodomains, ∼1−3 nm in diameter, due to the chemical incompatibility of its two components and its molecular architecture.

PVDF and PEGPEA microphase-separate given the large difference between their solubility parameters δ,[48] used to predict polymer miscibility, and correlated with the Flory−Huggins interaction parameter, χ:[49]

$$\chi = \frac{V}{RT}(\delta_1 - \delta_2)^2 = \frac{V}{RT}\Delta\delta_{1,2}{}^2 \quad (2)$$

where T is the temperature, R is the gas constant, and V is the molar volume of the repeating unit[50] (116.6 cm^3/mol). Solubility parameters for PVDF and PEGPEA are 17.5 and 23.1 $MPa^{1/2}$, respectively.[48] This corresponds to χ = 1.5 for this polymer pair, a high value indicating they will be immiscible.[51,52]

We have verified microphase separation by differential scanning calorimetry (DSC) of the copolymer and relevant homopolymers (Figure 2a). PVDF-*g*-PEGPEA shows a glass-transition temperature (T_g) of ∼13 °C, matching that observed for PEGPEA homopolymer. The T_g for PVDF, expected around −35 °C,[53] was not observed, likely due to the temperature range of the instrument. The existence of PVDF domains is evidenced by the melting peak around 165 °C, observed in both P(VDF-*co*-CTFE) and PVDF-*g*-PEGPEA. PVDF domains are partially crystalline, ∼20% for P(VDF-*co*-CTFE) and 10% for PVDF-*g*-PEGPEA.

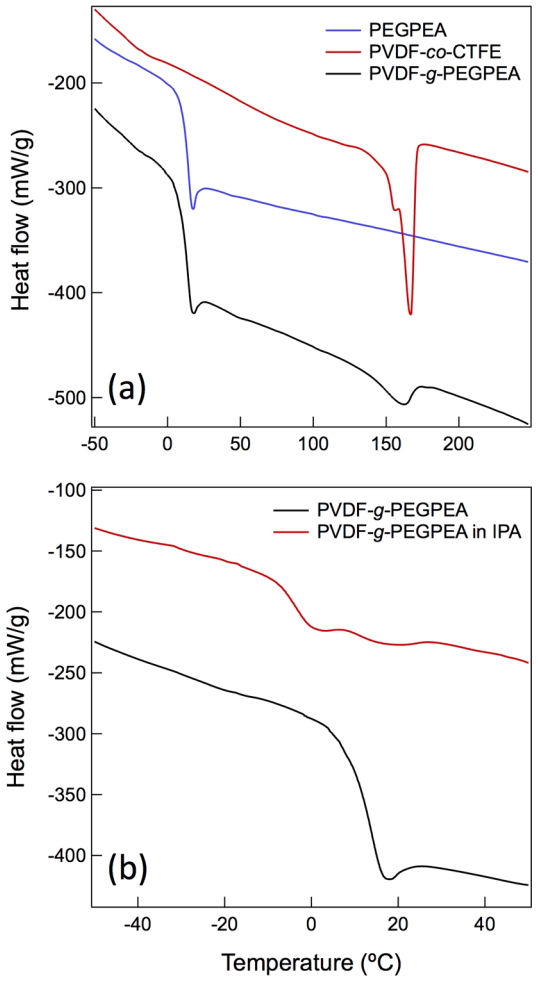

Figure 2. DSC thermograms of PEGPEA, PVDF-*co*-CTFE, PVDF-*g*-PEGPEA (a) and PVDF-*g*-PEGPEA with and without IPA (b). The heating rate is 10 °C/min.

Extensive literature shows that copolymers with comb architecture microphase-separate into network-type morphologies.[35,36,38,52,54,55] Approximately 50:50 volume ratios lead to bicontinuous networks of each domain. When the side chain is the majority component, a network of the side chain domains interspersed with backbone domains is observed.[36,38,52,54,55] The domain diameter is comparable with the side chain radius of gyration, R_g.[35] Based on this, we expect PVDF-*g*-PEGPEA to microphase separate to form PEGPEA nanodomains that form a network of "nanochannels" that span the material whose size scale is comparable with the R_g of the side chains.

The unperturbed root mean squared radius of gyration of a polymer R_g can be estimated by[56]

$$R_g = \sqrt{\frac{c_\infty n l^2}{6}} \quad (3)$$

where c_∞ is the characteristic ratio, n is the number of C−C bonds (20 for a 10-mer), and l is the C−C bond length (0.154 nm).[57] While we could not find the c_∞ value for PEGPEA, that of poly(ethylene glycol phenyl ether methacrylate) (PEGPEMA) is 16.19,[58] yielding an R_g of 1.13 nm. That of PEGPEA should be slightly lower. Even in an all-trans conformation, a 10-mer would have an end-to-end distance of 2.5 nm. Therefore, this copolymer is expected to form ∼1−3 nm PEGPEA domains, slightly larger than solute molecules.[35−38,48]

To characterize the nanostructure, small-angle X-ray scattering (SAXS) was performed on PVDF-*g*-PEGPEA using synchrotron X-rays at Kyushu University Beamline (Figure 3).

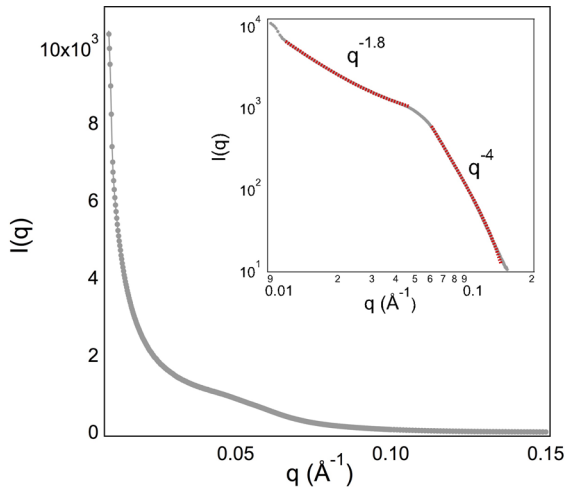

Figure 3. SAXS profile of PVDF-*g*-PEGPEA. Inset: same plot in log−log scale (Guinier-Porod analysis).

The pattern shows a small bump at q = 0.052 Å, corresponding to a characteristic length of ∼12 nm. We estimated the width of PEGPEA channels that correspond to this characteristic length to be 1.2−3.6 nm (Supporting Information), in agreement with the estimates from R_g.

Guinier-Porod analysis[59] (Figure 3, inset) shows power-law behavior with exponent 1.8 at low-q, which suggests a lamellar

DOI: 10.1021/acsmacrolett.5b00401
ACS Macro Lett. 2015, 4, 872−878

Table 1. Molecular Volume, Solubility Parameters, and Single-Solute Permeation Properties through Copolymer and Control Membranes of Five Solutes

				diffusion rate (10^{-10} mol/min)		permeability (10^{-11} m^2/s)		permeation selectivity with respect to MCH	
molecule	MV (Å^3)	δ (MPa$^{1/2}$)	$\Delta\delta$ (MPa$^{1/2}$)	copolymer	control	copolymer	control	copolymer	control
MCH[a]	125.5	16.1	7	0.15	0.13	0.28	7.1	1	1
PFS[b]	139.8	31.8	8.7	0.32	0.67	0.6	37	2	5
NB[a]	108	23.2	0.1	3.31	1.44	6.13	80	22	11
ANI[a]	109.8	26.3	3.2	2.21	1.53	4.09	85	15	12
DMNP[b]	182.2	26.4	3.3	1.66	0.15	3.07	8.4	11	1
PEGPEA		23.1							
PVDF		17.5							

[a]Concentration measured with GCMS. [b]Concentration measured with UV−visible spectrophotometry.

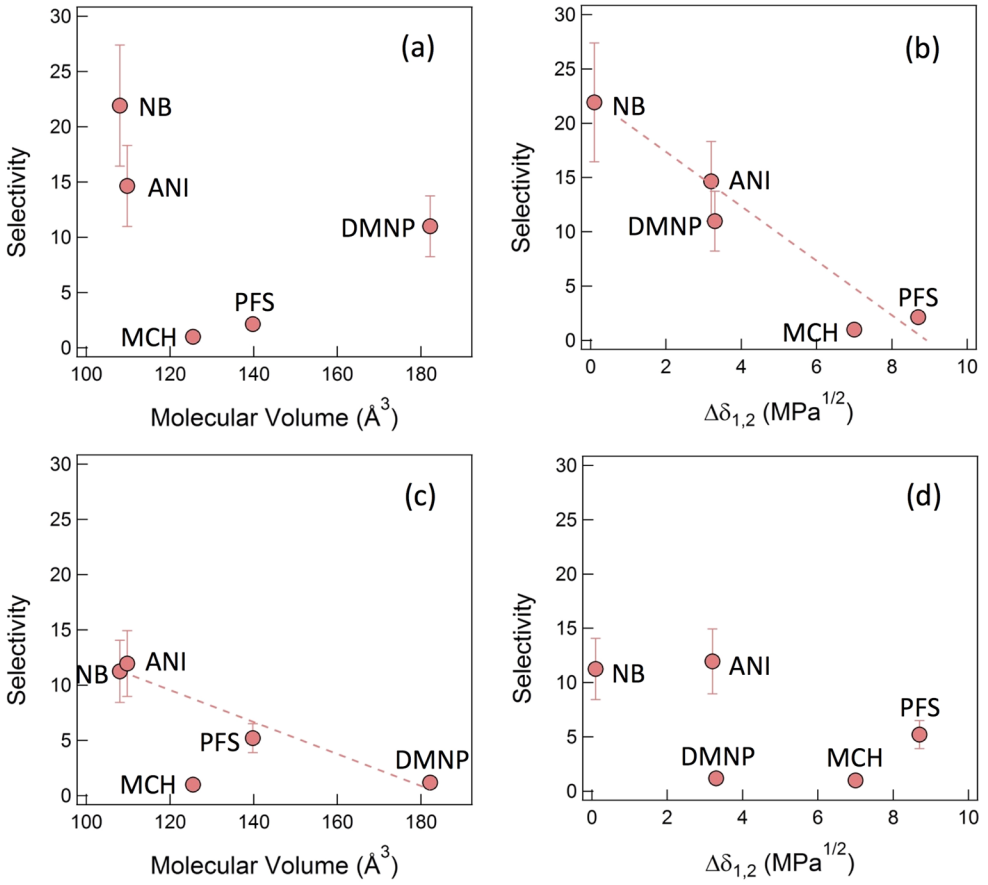

Figure 4. Single-solute diffusion rates vs molecular volume, MV (a−c) and solubility parameter difference between solute and PEGPEA, $\Delta\delta_{1,2}$ (b−d) for copolymer and control membranes. Dashed lines show linear regression of the data points. Error bars indicate average error margins (25%) from three measurements for each solute.

network structure.[60] At high-q, the pattern follows Porod's law indicating Gaussian chains within amorphous domains.[61,62] Overall, SAXS analysis supports a microphase-separated morphology with a continuous network of PEGPEA domains, interspersed with PVDF domains.[63] While it is hard to tell if PVDF domains are continuous, their presence is sufficient to form confined PEGPEA nanochannels.

We prepared ∼2 μm thick films, or dense membranes, of PVDF-*g*-PEGPEA by casting a 15 μm layer of a 15 wt % copolymer solution in DMF with a blade applicator and then soaking it in isopropanol. To serve as a control without microphase separated nanostructure, we prepared a ∼60 μm thick cross-linked PEGPEA film by photoinduced polymerization of a mixture of 16:1 EGPEA/poly(ethylene glycol) diacrylate (PEGDA, 258 g/mol) by weight. The solubility parameters of PEGDA and PEGPEA are similar, so no microphase separation is expected.

To observe nanoconfinement effects in the graft copolymer, the solvent needs to selectively swell PEGPEA but not PVDF, so that solutes permeate only through PEGPEA-filled "nanochannels".[36,64,65] Isopropanol was selected as the solvent because it swells PEGPEA but not PVDF based on literature,[65] solvent uptake, and diffusion experiments (not shown). DSC also supports the selective swelling of PEGPEA by IPA. Figure 2b shows that the T_g of PEGPEA shifts to lower temperature (−4 °C) if the copolymer is soaked in IPA before DSC analysis.

DOI: 10.1021/acsmacrolett.5b00401
ACS Macro Lett. 2015, 4, 872−878

Plasticization confirms IPA is preferentially swelling the PEGPEA domains.

We performed permeation experiments using a side-by-side diffusion cell to measure permeation rates (see Supporting Information for procedure). Solute concentration was measured by UV−visible spectroscopy or gas chromatography−mass spectroscopy (GCMS) and used to determine the mass transfer rate of the solute through the membrane. Single-solute permeation tests were run on six different molecules: nitrobenzene (NB), methylcyclohexane (MCH), 4-methylphenol (MP), anisole (ANI), pentafluorostyrene (PFS), and dimethoxy naphthalene (DMNP; Table 1). All molecules have similar diameters (5−6 Å).[36,37] All except MCH are aromatic and can interact with the aromatic groups of PEGPEA through π-stacking interactions.[55] The solutes have varying solubility parameters. Permeation rates and permeabilities (eq 1)[66] through PVDF-*g*-PEGPEA and cross-linked PEGPEA membranes are reported in Table 1, together with the molecular volume (MV, calculated using Molecular modeling Pro), and solubility parameter δ.[48]

We plotted our data in terms of permeation selectivity, R, by normalizing the permeability of each molecule, P_{mol} by that of a reference, P_{ref}.

$$R = \frac{P_{mol}}{P_{ref}} \tag{4}$$

We selected the lowest permeability solute, MCH, as the reference to emphasize the differences between the permeation rates of different molecules through each material. According to the solution-diffusion model, selectivity should not change upon the introduction of an impermeable phase.

We plotted permeation selectivities of different solutes versus solute molecular volume to indicate solute size, and the difference between the solubility parameters of the solute and PEGPEA, $\Delta\delta_{1,2}$, to indicate chemical affinity (Figure 4). Solutes with higher molecular volume will have lower diffusivity D_A. If this effect dominates, permeability and selectivity should decrease with increasing solute size. Solutes that preferentially interact with and partition into PEGPEA are expected to have smaller $\Delta\delta_{1,2}$ values (1, solute; 2, PEGPEA). If the separation is dominated by chemical structure differences, smaller $\Delta\delta_{1,2}$ values are expected to lead to increased permeability.

For the PVDF-*g*-PEGPEA copolymer membranes, there is no correlation between selectivity and molecular volume (Figure 4a). Instead, a strong correlation is observed between the permeation selectivities and $\Delta\delta_{1,2}$ (Figure 4b). Permeability decreases with increasing $\Delta\delta_{1,2}$, following an essentially linear trend. This indicates that PEGPEA−solute interactions are the dominant parameter determining solute permeability through this copolymer. No correlation is observed with $\Delta\delta_{1,2}$ when 1 = molecule and 2 = PVDF, further indicating that permeation occurs exclusively through PEGPEA domains.

The cross-linked PEGPEA control membrane shows distinctly different trends. There is a strong, roughly linear correlation between permeability and molecular volume (Figure 4c). Permeability is not correlated with $\Delta\delta_{1,2}$ (Figure 4d). In the absence of confining nanostructure, diffusion rates are dominated by solute size provided the solutes are sufficiently soluble.

This suggests that a microphase-separated nanostructure that confines permeation can lead to a significantly different permeation selectivity mechanism, increasing the influence of chemical structure effects (solubility, affinity) over that of solute size and diffusivity. By confining solute transport into functionalized nanochannels of size comparable to the solutes, a distinctly different basis of separation can be obtained.

Furthermore, higher diffusion selectivities are obtained in the nanostructured copolymer. This can be seen in single-solute experiments (Figure 4), but membrane selectivity can change upon exposure to more than one solute at a time.[11,15,67] We conducted competitive permeation experiments using feed solutions containing 1 mM of each of NB (aromatic) and MCH (nonaromatic; Figure 5). Despite comparable molecular

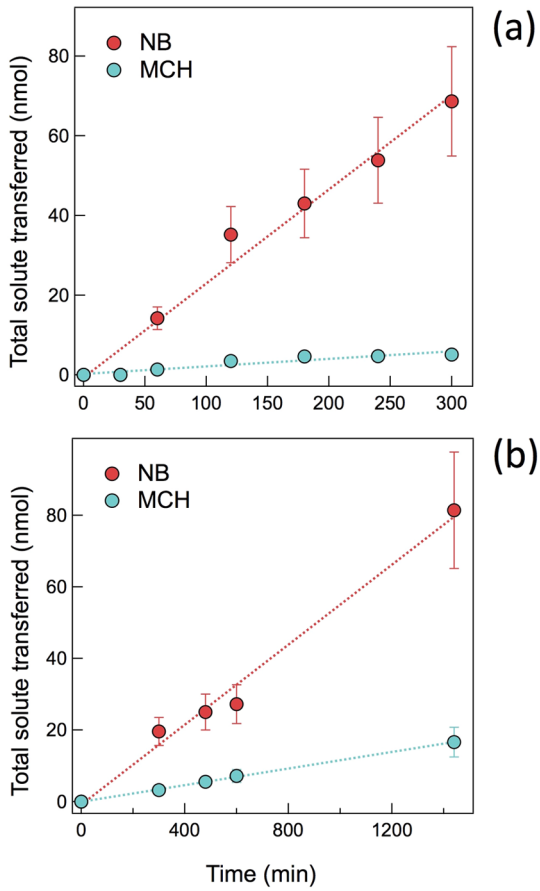

Figure 5. Diffusion rate of NB and MCH in competitive permeation experiments through PVDF-*g*-PEGPEA copolymer (a) and cross-linked PEGPEA control (b) membranes.

volumes, the permeation rate of NB ($2.5 \pm 0.9 \times 10^{-10}$ mol/min) through PVDF-*g*-PEGPEA is 15× higher than that of MCH ($1.6 \pm 0.7 \times 10^{-11}$ mol/min). The cross-linked PEGPEA control membrane shows a lower selectivity of 6. This shows that the nanostructure in PVDF-*g*-PEGPEA increases permeation selectivity due to aromaticity by confining flow and enhancing the effect of π-stacking interactions between PEGPEA and NB.

This study demonstrates that the confinement of the permeable polymer into a self-assembled nanostructure at a size scale that is comparable with solute size can significantly change which molecular parameters solute permeation rates correlate with. In the absence of nanoconfinement, smaller solutes diffuse faster. In contrast, in a microphase-separated copolymer that forms PEGPEA nanodomains through which permeation occurs, permeation rates show little correlation

DOI: 10.1021/acsmacrolett.5b00401
ACS Macro Lett. 2015, 4, 872−878

with solute size. Instead, permeation selectivity is strongly based on the solubility of solutes in PEGPEA. This is, to our knowledge, the first documentation of the effect of microphase-separated nanostructure on permeation selectivity and the distinct change in separation mechanisms. We believe that these initial insights will lead to a better understanding of how polymer self-assembly can be utilized to rationally design and create materials for various applications, from chemically selective membranes to barrier materials.

■ ASSOCIATED CONTENT

Supporting Information

Detailed experimental methods, solubility parameter estimation, and NMR, DSC, SEM, SAXS, and FTIR analyses. The Supporting Information is available free of charge on the ACS Publications website at DOI: 10.1021/acsmacrolett.5b00401.

(PDF)

■ AUTHOR INFORMATION

Corresponding Author

*E-mail: ayse.asatekin@tufts.edu.

Notes

The authors declare no competing financial interest.

■ ACKNOWLEDGMENTS

The authors thank Prof. Peggy Cebe for access to DSC, David Wilbur for help with GCMS analysis, and Tufts University for funding. SAXS experiments were carried out using the synchrotron X-rays at Kyushu University Beamline (SAGA-LS/BL06) with the proposal No. 2015IK001.

■ REFERENCES

(1) Xu, J. J.; Asatekin, A.; Gleason, K. K. *Adv. Mater.* **2012**, *24* (27), 3692−3696.
(2) Ranjan, S.; Dasgupta, N.; Chakraborty, A.; Melvin Samuel, S.; Ramalingam, C.; Shanker, R.; Kumar, A. *J. Nanopart. Res.* **2014**, *16* (6), 1−23.
(3) Lange, J.; Wyser, Y. *Packag. Technol. Sci.* **2003**, *16* (4), 149−158.
(4) Kumar, A.; Srivastava, A.; Galaev, I. Y.; Mattiasson, B. *Prog. Polym. Sci.* **2007**, *32* (10), 1205−1237.
(5) Yoshida, M.; Langer, R.; Lendlein, A.; Lahann, J. *J. Macromol. Sci., Polym. Rev.* **2006**, *46* (4), 347−375.
(6) LaVan, D. A.; McGuire, T.; Langer, R. *Nat. Biotechnol.* **2003**, *21* (10), 1184−1191.
(7) Baxamusa, S. H.; Montero, L.; Dubach, J. M.; Clark, H. A.; Borros, S.; Gleason, K. K. *Biomacromolecules* **2008**, *9* (10), 2857−2862.
(8) Lakshmi, B. B.; Martin, C. R. *Nature* **1997**, *388*, 758−760.
(9) Lee, S. B.; Mitchell, D. T.; Trofin, L.; Nevanen, T. K.; Soderlund, H.; Martin, C. R. *Science* **2002**, *296*, 2198−2200.
(10) Kohli, P.; Harrell, C. C.; Cao, Z.; Gasparac, R.; Tan, W.; Martin, C. R. *Science* **2004**, *305*, 984.
(11) Baker, R. W. *Membrane Technology and Applications*, 2nd ed.; J. Wiley: Chichester; New York, 2004; p *x*.
(12) Freeman, B. D.; Pinnau, I. *Trends Polym. Sci.* **1997**, *5* (5), 167−173.
(13) Freeman, B. D., Pinnau, I., Eds. *Polymer Membranes for Gas and Vapor Separation: Chemistry and Materials Science*; American Chemical Society: Washington, DC, 1999; p x.
(14) Javaid, A. *Chem. Eng. J.* **2005**, *112* (1−3), 219−226.
(15) Freeman, B.; Pinnau, I. *Trends Polym. Sci.* **1997**, *5* (5), 167−173.
(16) Geise, G. M.; Doherty, C. M.; Hill, A. J.; Freeman, B. D.; Paul, D. R. *J. Membr. Sci.* **2014**, *453* (0), 425−434.
(17) Geise, G. M.; Freeman, B. D.; Paul, D. R. *J. Membr. Sci.* **2013**, *427*, 186−196.
(18) Zeth, K.; Thein, M. *Biochem. J.* **2010**, *431*, 13−22.
(19) Kowalczyk, S. W.; Kapinos, L.; Blosser, T. R.; Magalhaes, T.; van Nies, P.; Lim, R. Y.; Dekker, C. *Nat. Nanotechnol.* **2011**, *6* (7), 433−8.
(20) Friedman, M. H. *Principles and Models of Biological Transport*; Springer: New York, NY, 2008; p *xvii*.
(21) DeLano, W. L.; Ultsch, M. H.; De Vos, A. M.; Wells, J. A. *Science* **2000**, *287*, 1279−1284.
(22) Berg, T. *Angew. Chem., Int. Ed.* **2003**, *42*, 2462−2481.
(23) Jirage, K. B.; Hulteen, J. C.; Martin, C. R. *Science* **1997**, *278*, 655−658.
(24) Wirtz, M.; Yu, S. F.; Martin, C. R. *Analyst* **2002**, *127* (7), 871−879.
(25) Velleman, L.; Triani, G.; Evans, P. J.; Shapter, J. G.; Losic, D. *Microporous Mesoporous Mater.* **2009**, *126* (1−2), 87−94.
(26) Escobar, C.; Zulkifli, A.; Faulkner, C. J.; Trzeciak, A.; Jennings, G. K. *ACS Appl. Mater. Interfaces* **2012**, *4*, 906−915.
(27) Savariar, E. N.; Krishnamoorthy, K.; Thayumanavan, S. *Nat. Nanotechnol.* **2008**, *3* (2), 112−7.
(28) Asatekin, A.; Gleason, K. K. *Nano Lett.* **2011**, *11* (2), 677−86.
(29) Asatekin, A.; Vannucci, C. *Nanosci. Nanotechnol. Lett.* **2015**, *7* (1), 21−32.
(30) Park, C.; Yoon, J.; Thomas, E. L. *Polymer* **2003**, *44* (22), 6725−6760.
(31) Schacher, F. H.; Rupar, P. A.; Manners, I. *Angew. Chem., Int. Ed.* **2012**, *51* (32), 7898−7921.
(32) Yang, S. Y.; Ryu, I.; Kim, H. Y.; Kim, J. K.; Jang, S. K.; Russell, T. P. *Adv. Mater.* **2006**, *18* (6), 709−712.
(33) Grozea, C. M.; Li, I. T. S.; Grozea, D.; Walker, G. C. *Macromolecules* **2011**, *44* (10), 3901−3909.
(34) Luo, M.; Epps, T. H. *Macromolecules* **2013**, *46* (19), 7567−7579.
(35) Foster, D. P.; Jasnow, D.; Balazs, A. C. *Macromolecules* **1995**, *28* (9), 3450−3462.
(36) Asatekin, A.; Olivetti, E. A.; Mayes, A. M. *J. Membr. Sci.* **2009**, *332* (1−2), 6−12.
(37) Bengani, P.; Asatekin, A. *J. Membr. Sci.* **2015**, *493*, 755−765.
(38) Akthakul, A.; Salinaro, R. F.; Mayes, A. M. *Macromolecules* **2004**, *37* (20), 7663−7668.
(39) Matyjaszewski, K.; Tsarevsky, N. V. *Nat. Chem.* **2009**, *1* (4), 276−288.
(40) Ahn, S. H.; Koh, J. H.; Seo, J. A.; Kim, J. H. *Chem. Commun.* **2010**, *46*, 1935−1937.
(41) Nedelcu, M.; Lee, J.; Crossland, E. J. W.; Warren, S. C.; Orilall, M. C.; Guldin, S.; Hüttner, S.; Ducati, C.; Eder, D.; Wiesner, U. *Soft Matter* **2009**, *5*, 134−139.
(42) Zilman, A.; Di Talia, S.; Jovanovic-Talisman, T.; Chait, B. T.; Rout, M. P.; Magnasco, M. O. *PLoS Comput. Biol.* **2010**, *6* (6), e1000804.
(43) Davis, K. A.; Matyjaszewski, K. *Adv. Polym. Sci.* **2002**, *159*, 108.
(44) Matyjaszewski, K.; Xia, J. *Chem. Rev.* **2001**, *101* (9), 2921−2990.
(45) Udding, J. H.; Tuijp, K. C. J. M.; Van Zanden, M. N. A.; Hiemstra, H.; Speckamp, W. N. *J. Org. Chem.* **1944**, *59* (8), 1993−2003.
(46) Zhang, M. F.; Russell, T. P. *Macromolecules* **2006**, *39* (10), 3531−3539.
(47) Chen, J.; Tan, S.; Gao, G.; Li, H.; Zhang, Z. *Polym. Chem.* **2014**, *5* (6), 2130.
(48) Van Krevelen, D. W.; Te Nijenhuis, K. *Properties of Polymers: Their Correlation with Chemical Structure; Their Numerical Estimation and Prediction from Additive Group Contributions*; Elsevier Science: New York, 1972.
(49) Hildebrand, J. H.; Scott, R. L. *The Solubility of Nonelectrolytes*; Van Nostrand-Reinhold: Princeton, NJ, 1950.
(50) David, D. J.; Sincock, T. J. *Polymer* **1992**, *33* (21), 4505−4514.
(51) Pospiech, D.; Gottwald, A.; Jehnichen, D.; Friedel, P.; John, A.; Harnisch, C.; Voigt, D.; Khimich, G.; Bilibin, A. *Colloid Polym. Sci.* **2002**, *280* (11), 1027−1037.
(52) Chi, W. S.; Hong, S. U.; Jung, B.; Kang, S. W.; Kang, Y. S.; Kim, J. H. *J. Membr. Sci.* **2013**, *443*, 54−61.

DOI: 10.1021/acsmacrolett.5b00401
ACS Macro Lett. 2015, 4, 872−878

(53) Bonardelli, P.; Moggi, G.; Turturro, A. *Polymer* **1986**, *27* (6), 905−909.
(54) Shinozaki, A.; Jasnow, D.; Balazs, A. C. *Macromolecules* **1994**, *27* (9), 2496−2502.
(55) Hester, J. F.; Olugebefola, S. C.; Mayes, A. M. *J. Membr. Sci.* **2002**, *208* (1−2), 375−388.
(56) Rodriguez, F. *Principles of Polymer Systems*; McGraw-Hill Books: New York, 1982; pp 157−162.
(57) Young, R. J.; Lovell, P. *Introduction to Polymers*, 2nd ed.; Chapman and Hall: London; New York, 1991; p *x*.
(58) Safranski, D. L. *Effect of Chemical Structure and Crosslinking Density on the Thermomechanical Properties and Toughness of Meth(acrylate) Shape-Memory Polymer Networks*; Georgia Institute of Technology: Atlanta, GA, 2008.
(59) Hammouda, B. *J. Appl. Crystallogr.* **2010**, *43* (4), 716−719.
(60) Roe, R. *Methods of X-ray and Neutron Scattering in Polymer Science*; Oxford University Press: New York, 2000.
(61) Beaucage, G.; Schaefer, D. W. *J. Non-Cryst. Solids* **1994**, *172*−*174*, 797−805.
(62) Benoit, H.; Joanny, J. F.; Hadziioannou, G.; Hammouda, B. *Macromolecules* **1993**, *26*, 5790.
(63) Miyata, T.; Obata, S.; Uragami, T. *Macromolecules* **1999**, *32*, 3712−3720.
(64) Akthakul, A.; Hochbaum, A. I.; Stellacci, F.; Mayes, A. M. *Adv. Mater.* **2005**, *17* (5), 532−535.
(65) Asatekin, A.; Mayes, A. M. *Sep. Sci. Technol.* **2009**, *44* (14), 3330−3345.
(66) Crank, J.; Park, G. S. *Diffusion in Polymers*; Academic Press: New York, 1968.
(67) Zilman, A.; Di Talia, S.; Jovanovic-Talisman, T.; Chait, B. T.; Rout, M. P.; Magnasco, M. O. *PLoS Comput. Biol.* **2010**, *6* (6), e1000804.

DOI: 10.1021/acsmacrolett.5b00401
ACS Macro Lett. 2015, 4, 872−878